JOURNAL OF OPTOELECTRONICS AND ADVANCED MATERIALS Vol. 9, No. 4, April 2007, p. 1091 - 1103

The influence of fabrication errors and periodic defects on the width and number of 1D photonic crystals band gaps

B. LAZAR, P. STERIAN*
University Center for Optical Engineering and Photonics, Bucharest Polytechnic University, 76206 Bucharest, Romania

With the help of periodic defects tiny allowed spaces of frequency can be introduced in the middle of the forbidden domains belonging to the perfect, unperturbed 1D crystal (without impurities). A 1D photonic crystal is relatively resistant to fabrication errors, the band gaps maintaining their position and width even if the manufacturing tolerance is large enough.

(Received November 2, 2006; accepted February 28, 2007)

Keywords: 1D photonic crystal, Fabrication errors, Band gaps

1. Introduction

Photonic crystals are periodic structures consisting of alternating regions with different refractive indices. Their design represents, in most of the cases, a challenging task because of fine details that are smaller than the utilized wavelength, while the total structure extends usually over regions significantly larger than a wavelength. In principle the evaluation of their properties can be done with the help of computer simulations but there is no simple approach for the problem [1]. An ordinary personal computer has serious limitations even if it is used for simple tasks like obtaining the band structure of bidimensional crystals, supposed to be perfectly periodic and having elementary cells that do not involve an exaggerated number of discretization elements, a fact that is valid in general for 2D structures without periodic defects and fabrication errors. If these two last design parameters are taken into account, 2D algorithms implemented on PCs become impractical and a supercomputer needs to be used [2], [3]. Such a device is not largely available and just a few people can afford to use one. Fortunately, this is not the case of 1D crystals where both the influence of errors and periodic impurities can by studied [5] employing just normal computers.

The goal of the present paper is to implement and utilize an 1D algorithm able to predict changes in the band structure when the periodicity of the photonic crystal is perturbed either by random inhomogeneities or periodic defects.

2. Theoretical presentation

Generally, a multilayer periodic structure, named also 1D photonic crystal can be schematically described by the representation in Fig. 1.

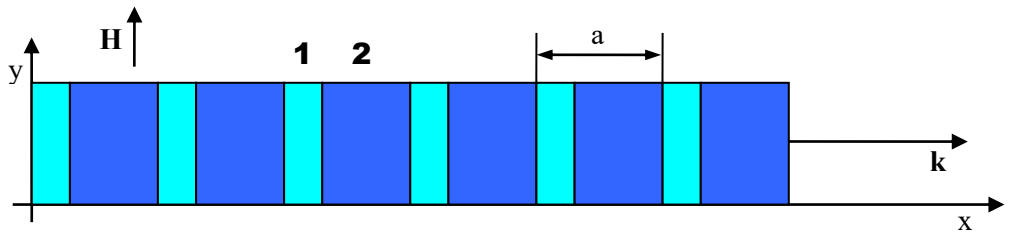

Fig. 1. Multilayer structure, named also one dimensional photonic crystal.

The dielectric layers *1* and *2* are considered unbounded on *y* and z. The structure has periodicity only along the *x* axis. Regarding the electromagnetic field, it is supposed to by linearly polarized, having the **H** component parallel to the *y* direction. The field propagates along *x*.

Generally speaking, the propagation of electromagnetic waves in a medium with 3D periodicity is governed by the following equation:

$$\text{(a)}\ \nabla\times\left(\frac{1}{\varepsilon_r(\mathbf{r})}\nabla\times\mathbf{H}(\mathbf{r})\right)=\frac{\omega^2}{c^2}\mathbf{H}(\mathbf{r})\ \text{or equivalent}$$

$$\text{(b)}\ \frac{1}{\varepsilon_r(\mathbf{r})}(\nabla\times[\nabla\times\mathbf{E}(\mathbf{r})])=\frac{\omega^2}{c^2}\mathbf{E}(\mathbf{r}) \qquad (1)$$

which can be quickly derived from Maxwell equations.
For one dimensional case the entity (1) (a) has to by reduced to its particular 1D form. Therefore, first of all,

the expression of the quantity $\nabla\times\left[(1/\varepsilon_r(\mathbf{r}))\nabla\times\mathbf{H}(\mathbf{r})\right]$ where $\mathbf{H}(\mathbf{r})=0\cdot\mathbf{e}_x+H_y(x,y,z)\cdot\mathbf{e}_y+0\cdot\mathbf{e}_z$. must be found. Thus,

$$\nabla\times\mathbf{H}(\mathbf{r})=\left(\frac{\partial H_z}{\partial y}-\frac{\partial H_y}{\partial z}\right)\cdot\mathbf{e}_x+\left(\frac{\partial H_x}{\partial z}-\frac{\partial H_z}{\partial x}\right)\cdot\mathbf{e}_y+\left(\frac{\partial H_y}{\partial x}-\frac{\partial H_x}{\partial y}\right)\cdot\mathbf{e}_z=\frac{\partial H_y}{\partial x}\cdot\mathbf{e}_z \tag{2}$$

By applying once again the curl operator to (2) multiplied by $1/\varepsilon_r(\mathbf{r})$, the following expression results:

$$\nabla\times\left(\frac{1}{\varepsilon_r(\mathbf{r})}\nabla\times\mathbf{H}(\mathbf{r})\right)=-\frac{\partial}{\partial x}\left(\frac{1}{\varepsilon_r(x)}\frac{\partial H_y}{\partial x}\right)\cdot\mathbf{e}_y=-\frac{\partial}{\partial x}\left(\frac{1}{\varepsilon_r(x)}\right)\frac{\partial H_y}{\partial x}\cdot\mathbf{e}_y-\frac{1}{\varepsilon_r(x)}\frac{\partial H_y^2}{\partial x^2}\cdot\mathbf{e}_y \tag{1}$$

Finally the 1D equivalent of (1) is obtained as being:

$$-\frac{\partial}{\partial x}\left(\frac{1}{\varepsilon_r(x)}\right)\frac{\partial H_y(x)}{\partial x}-\frac{1}{\varepsilon_r(x)}\frac{\partial H_y^2(x)}{\partial x^2}=\frac{\omega^2}{c^2}H_y(x) \tag{4}$$

However, the expression (4) is complicated enough. For this reason, the equivalent in E in preferred. The link between **E** and **H** (in general) is given by the relation: $\nabla\times\mathbf{H}=\varepsilon_0\varepsilon_r(\mathbf{r})\frac{\partial\mathbf{E}}{\partial t}$. If **E**, **H** are armonic then:

$$\frac{\partial H_y(x)}{\partial x}\cdot\mathbf{e}_z e^{j\omega t}=j\omega\varepsilon_0\varepsilon_r(x)E(x)e^{j\omega t}\ \Rightarrow\ E_z(x)=\frac{jke^{jkx}u(x)+e^{jkx}\frac{\partial u(x)}{\partial x}}{j\omega\varepsilon_0\varepsilon_r(x)}=e^{jkx}\underbrace{\frac{ku(x)-j\frac{\partial u(x)}{\partial x}}{\omega\varepsilon_0\varepsilon_r(x)}}_{\substack{not\\ g(x)}} \tag{5}$$

where $g(x)$ is a repetitive function having the period equal with the one of the 1D crystal. In (5) it was taken into account that, for the general case (field propagation inside a periodic medium), $\mathbf{H}(\mathbf{r})=e^{j\mathbf{k}\cdot\mathbf{r}}u(\mathbf{r})$ where $u(\mathbf{r})$ is periodic with $u(\mathbf{r})=u(\mathbf{r}+\mathbf{a})$, **a** being the spatial period [Bloch-Floquet theorem].

So, from (5) it follows that **E** is parallel to z and can be written, similar to **H,** like a product between e^{jkx} and a repetitive function having the period a.

Therefore, $\mathbf{E}(\mathbf{r})=0\cdot\mathbf{e}_x+0\cdot\mathbf{e}_y+E_z(x,y,z)\cdot\mathbf{e}_z$ and (1) (b) becomes:

$$-\frac{1}{\varepsilon_r(x)}\frac{\partial E_z^2(x)}{\partial x^2}=\frac{\omega^2}{c^2}E_z(x);\ \text{with}\ \varepsilon_r(x)=\varepsilon_r(x+a),\quad g(x)=g(x+a),\ E(x)=e^{jkx}g(x) \tag{6}$$

(6) in equivalent with (4) but having a simpler form is preferred in the calculations that follows:

As ε_r is periodic, $\varepsilon_r^{-1}(x)$ is also repetitive, and has a Fourier expansion:

$$\varepsilon_r^{-1}(x)=\sum_{n=-\infty}^{\infty}p_n e^{j\frac{2\pi n}{a}x} \tag{7}$$

where p_n are the coefficients of the sum which can be calculated directly due to the fact that $\varepsilon_r(x)$ is known.

Similar with $\varepsilon_r^{-1}(x)$, $E(x)=e^{jkx}g(x)$ can be written as:

$$E(x)=\sum_{m=-\infty}^{\infty}h_m e^{j\left(k+\frac{2\pi m}{a}\right)x}\ ,\ h_m \text{ being the Fourier coefficients.} \tag{8}$$

By replacing (7), (8) in (6) the following equation results:

$$\left(\sum_{n=-\infty}^{\infty}p_n e^{j\frac{2\pi n}{a}x}\right)\left(\sum_{m=-\infty}^{\infty}h_m\left(k+\frac{2\pi m}{a}\right)^2 e^{j\left(k+\frac{2\pi m}{a}\right)x}\right)=\frac{\omega^2}{c^2}\sum_{m=-\infty}^{\infty}h_m e^{j\left(k+\frac{2\pi m}{a}\right)x}, \tag{9}$$

that can be further simplified to:

$$\sum_{n=-\infty}^{\infty}\sum_{m=-\infty}^{\infty}h_m p_n\left(k+\frac{2\pi m}{a}\right)^2 e^{j\frac{2\pi(m+n)}{a}x}=\frac{\omega^2}{c^2}\sum_{m=-\infty}^{\infty}h_m e^{j\frac{2\pi m}{a}x} \tag{10}$$

If both left and right members of the (10) eq. are multiplied by $(1/a)e^{-j(2\pi/a)m'x}$ and integrated in respect to x, it follows that:

$$\sum_{n=-\infty}^{\infty}\sum_{m=-\infty}^{\infty}h_m p_n\left(k+\frac{2\pi m}{a}\right)^2\frac{1}{a}\int_{-\frac{a}{2}}^{\frac{a}{2}}e^{j\frac{2\pi(m+n)}{a}x}e^{-j\frac{2\pi m'}{a}x}dx=\frac{\omega^2}{c^2}\sum_{m=-\infty}^{\infty}h_m\frac{1}{a}\int_{-\frac{a}{2}}^{\frac{a}{2}}e^{j\frac{2\pi m}{a}x}e^{-j\frac{2\pi m'}{a}x}dx \tag{11}$$

which, in its turn, becomes:

$$\sum_{n=-\infty}^{\infty}\sum_{m=-\infty}^{\infty}h_m p_n\left(k+\frac{2\pi m}{a}\right)^2\underbrace{\frac{\sin[\pi(m+n-m')]}{\pi(m+n-m')}}_{\delta_{m+n,m'}}=\frac{\omega^2}{c^2}\sum_{m=-\infty}^{\infty}h_m\underbrace{\frac{\sin[\pi(m-m')]}{\pi(m-m')}}_{\delta_{m,m'}} \tag{12}$$

For an arbitrary m', the majority of the terms on both sides of the equal sing, disappear (12) turns into:

$$\sum_{m=-\infty}^{\infty}h_m p_{m'-m}\underbrace{\left(k+\frac{2\pi m}{a}\right)^2}_{\substack{not\\ s_m}}=\frac{\omega^2}{c^2}h_{m'} \tag{13}$$

For practical calculations (13) will be truncated so that m, $m'\in[-M, M]$ where M is a positive integer. For each of the 2M+1 values of m' an equation like (13) is obtained, the coefficients $p_{m-m'}$ having indices which vary in the interval $[-2M, 2M]$:

$$\begin{cases} p_0 s_{-M} h_{-M} + \cdots + p_{-M+2} s_{-2} h_{-2} + p_{-M+1} s_{-1} h_{-1} + p_{-M} s_0 h_0 + p_{-M-1} s_1 h_1 + p_{-M-2} s_2 h_2 + \cdots + p_{-2M} s_M h_M = \dfrac{\omega^2}{c^2} h_{-M} \\ \vdots \\ p_{-2+M} s_{-M} h_{-M} + \cdots + p_0 s_{-2} h_{-2} + p_{-1} s_{-1} h_{-1} + p_{-2} s_0 h_0 + p_{-3} s_1 h_1 + p_{-4} s_2 h_2 + \cdots + p_{-2-M} s_M h_M = \dfrac{\omega^2}{c^2} h_{-2} \\ p_{-1+M} s_{-M} h_{-M} + \cdots + p_1 s_{-2} h_{-2} + p_0 s_{-1} h_{-1} + p_{-1} s_0 h_0 + p_{-2} s_1 h_1 + p_{-3} s_2 h_2 + \cdots + p_{-1-M} s_M h_M = \dfrac{\omega^2}{c^2} h_{-1} \\ p_M s_{-M} h_{-M} + \cdots + p_2 s_{-2} h_{-2} + p_1 s_{-1} h_{-1} + p_0 s_{0,0} h_0 + p_{-1} s_{1,0} h_1 + p_{-2} s_2 h_2 + \cdots + p_M s_M h_M = \dfrac{\omega^2}{c^2} h_0 \\ p_{1+M} s_{-M} h_{-M} + \cdots + p_3 s_{-2} h_{-2} + p_2 s_{-1} h_{-1} + p_1 s_0 h_0 + p_0 s_1 h_1 + p_{-1} s_2 h_2 + \cdots + p_{1-M} s_M h_M = \dfrac{\omega^2}{c^2} h_1 \\ p_{2+M} s_{-M} h_{-M} + \cdots + p_4 s_{-2} h_{-2} + p_3 s_{-1} h_{-1} + p_2 s_0 h_0 + p_1 s_1 h_1 + p_0 s_2 h_2 + \cdots + p_{2-M} s_M h_M = \dfrac{\omega^2}{c^2} h_2 \\ \vdots \\ p_{2M} s_{-M} h_{-M} + \cdots + p_{M+2} s_{-2} h_{-2} + p_{M+1} s_{-1} h_{-1} + p_M s_0 h_0 + p_{M-1} s_1 h_1 + p_{M-2} s_2 h_2 + \cdots + p_0 s_M h_M = \dfrac{\omega^2}{c^2} h_M \end{cases} \tag{14}$$

By making the notations:

$$\begin{pmatrix} p_0 s_{-M} & \cdots & p_{-M+2} s_{-2} & p_{-M+1} s_{-1} & p_{-M} s_0 & p_{-M-1} s_1 & p_{-M-2} s_2 & \cdots & p_{-2M} s_M \\ \vdots & & \vdots & & & & \vdots & & \vdots \\ p_{-2+M} s_{-M} & \cdots & p_0 s_{-2} & p_{-1} s_{-1} & p_{-2} s_0 & p_{-3} s_1 & p_{-4} s_2 & \cdots & p_{-2-M} s_M \\ p_{-1+M} s_{-M} & & p_1 s_{-2} & p_0 s_{-1} & p_{-1} s_0 & p_{-2} s_1 & p_{-3} s_2 & & p_{-1-M} s_M \\ p_M s_{-M} & & p_2 s_{-2} & p_1 s_{-1} & p_0 s_0 & p_{-1} s_1 & p_{-2} s_2 & & p_{-M} s_M \\ p_{1+M} s_{-M} & & p_3 s_{-2} & p_2 s_{-1} & p_1 s_0 & p_0 s_1 & p_{-1} s_2 & & p_{1-M} s_M \\ p_{2+M} s_{-M} & \cdots & p_4 s_{-2} & p_3 s_{-1} & p_2 s_0 & p_1 s_1 & p_0 s_2 & \cdots & p_{2-M} s_M \\ \vdots & & \vdots & & & & \vdots & & \vdots \\ p_{2M} s_{-M} & \cdots & p_{M+2} s_{-2} & p_{M+1} s_{-1} & p_M s_0 & p_{M-1} s_1 & p_{M-2} s_2 & \cdots & p_0 s_M \end{pmatrix} \overset{not}{=} \mathbf{S} \quad \text{and} \quad \begin{pmatrix} h_{-M} \\ h_{-M+1} \\ \vdots \\ h_{M-1} \\ h_M \end{pmatrix} \overset{not}{=} \mathbf{h} \tag{15}$$

it follows that:

$$\mathbf{S} \cdot \mathbf{h} = \frac{\omega^2}{c^2} \mathbf{h} \tag{16}$$

The equality (16) is fulfilled independently of the unknowns $h_{m'}$, if the quantity ω^2/c^2 is equal to one of the eigenvalues of the matrix **S**, where s_m can by calculated from (17) and the coefficients $p_{m-m'}$ are found by solving the system in (17).

Summarizing, for graphical representations of the function $\omega=\omega(k)$, the eigenvalues corresponding to a great number of **S** matrixes have to be evaluated for many k uniformly distributed in the interval $k\in[-\pi/a, \pi/a]$. It has to be noted that, in order to make the graphical diagrams more universal, a normalization is needed for both axes. Thus on x, k will be replaced by $ka/2\pi \in[-0.5, 0.5]$ and on y, ω will by divided by $2\pi c/a$ which, in fact, represents the pulsation of a reference radiation having the wavelength equal to a (the period of the crystal) that travel with the speed of light, c. In such a way, a more intuitive image of the band gaps size is created and the properties of various 1D periodic structures can be compared much easily.

$$\begin{pmatrix} e^{j\frac{4\pi(-M)}{a}\cdot 0} & e^{j\frac{2\pi(-2M+1)}{a}\cdot 0} & e^{j\frac{2\pi(-2M+2)}{a}\cdot 0} & & e^{j\frac{2\pi(2M-2)}{a}\cdot 0} & e^{j\frac{2\pi(2M-1)}{a}\cdot 0} & e^{j\frac{4M\pi}{a}\cdot 0} \\ e^{j\frac{4\pi(-M)}{ad^{-1}}} & e^{j\frac{2\pi(-2M+1)}{ad^{-1}}} & e^{j\frac{2\pi(-2M+2)}{ad^{-1}}} & \cdots & e^{j\frac{2\pi(2M-2)}{ad^{-1}}} & e^{j\frac{2\pi(2M-1)}{ad^{-1}}} & e^{j\frac{4M\pi}{ad^{-1}}} \\ e^{j\frac{4\pi(-M)}{ad^{-1}}} & e^{j\frac{2\pi(-2M+1)}{ad^{-1}}} & e^{j\frac{2\pi(-2M+2)}{ad^{-1}}} & & e^{j\frac{2\pi(2M-2)}{ad^{-1}}} & e^{j\frac{2\pi(2M-1)}{ad^{-1}}} & e^{j\frac{4M\pi}{ad^{-1}}} \\ \vdots & & & & & \vdots & \\ e^{j\frac{4\pi(-M)}{a(a-3d)^{-1}}} & e^{j\frac{2\pi(-2M+1)}{a(a-3d)^{-1}}} & e^{j\frac{2\pi(-2M+2)}{a(a-3d)^{-1}}} & & e^{j\frac{2\pi(2M-2)}{a(a-3d)^{-1}}} & e^{j\frac{2\pi(2M-1)}{a(a-3d)^{-1}}} & e^{j\frac{4M\pi}{a(a-3d)^{-1}}} \\ e^{j\frac{4\pi(-M)}{a(a-2d)^{-1}}} & e^{j\frac{2\pi(-2M+1)}{a(a-2d)^{-1}}} & e^{j\frac{2\pi(-2M+2)}{a(a-2d)^{-1}}} & \cdots & e^{j\frac{2\pi(2M-2)}{a(a-2d)^{-1}}} & e^{j\frac{2\pi(2M-1)}{a(a-2d)^{-1}}} & e^{j\frac{4M\pi}{a(a-2d)^{-1}}} \\ e^{j\frac{4\pi(-M)}{a(a-d)^{-1}}} & e^{j\frac{2\pi(-2M+1)}{a(a-d)^{-1}}} & e^{j\frac{2\pi(-2M+2)}{a(a-d)^{-1}}} & & e^{j\frac{2\pi(2M-2)}{a(a-d)^{-1}}} & e^{j\frac{2\pi(2M-1)}{a(a-d)^{-1}}} & e^{j\frac{4M\pi}{a(a-d)^{-1}}} \end{pmatrix} \begin{pmatrix} p_{-2M} \\ p_{-2M+1} \\ p_{-2M+2} \\ \\ p_{2M-2} \\ p_{2M-1} \\ p_{2M} \end{pmatrix} = \begin{pmatrix} \varepsilon^{-1}(0) \\ \varepsilon^{-1}(d) \\ \varepsilon^{-1}(2d) \\ \\ \varepsilon^{-1}(a-3d) \\ \varepsilon^{-1}(a-2d) \\ \varepsilon^{-1}(a-d) \end{pmatrix} \tag{17}$$

where $d=a/(4M+1)$.

3. The contrast and filling factor, two parameters that strongly influence the width and number of photonic band gaps. Numerical analysis

The expressions obtained in the previous paragraph (i.e: eq. (13) and the afferent relations) are directly implementable in computers, using a software mathematical tool like Matlab 6.5. Despite the fact that many numerical calculations have to be done, the overall process is manageable and an ordinary PC can fulfill the task in relatively short times. This is extremely important because studying (for the 1D case), the influence of the filling factor on the size of the gaps and on their number, gives important information about the behavior of similar 2D and 3D structures which can by hardly analyzed using normal computers. Also, the performances of bidimensional crystals can be partially investigated using a 2D generalization of (13), the 3D extension belonging to the same formula leads to intensive computational algorithms that surpass the power of modern PCs. Coming back to 2D crystals, it must be said that, studies regarding the influence of factors like filling coefficient or contrast can be directly analyzed using the 2D generalization of (13). However, this is true only makin the supposition of perfect periodic structures having elementary cells that do not involve exaggerated number of discretization elements, a fact that is valid in general for 2D crystals without periodic defects and fabrication errors. If these two last facts are taken into account the 2D generalization of (13) become impractical and a supercomputer have to be employed. However, this is not the case of 1D crystals where both the influence of errors and periodic impurities can by studied using PCs.

Also, the main goal of the paper is focused on errors and periodic defects, for comparison purposes, first of all the influence of the contrast and filling factor over the size of band gaps will be evaluated. The physical structure considered looks like the one in Fig. 1.

As the contrast increases the number of gaps is lower and lower but their width (and this is very important) grows considerably.

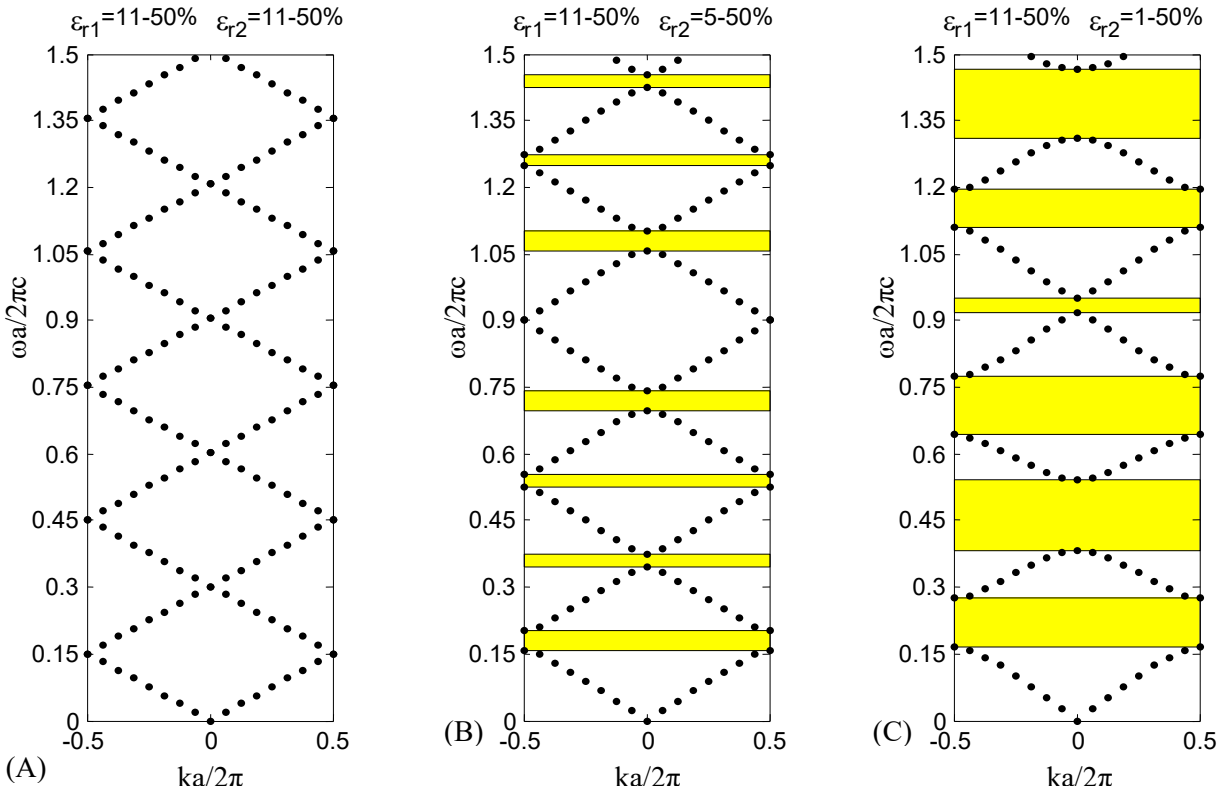

Fig. 2. (A). The band structure of a homogeneous medium having ε_r=11. There are no forbidden domains. (B) The band gaps of a multilayer with two alternating strata: ε_{r1}=11 and ε_{r2}=5. (C) The bands profile for the case where the two substances are characterized by: ε_{r1}=11 and ε_{r2}=1. The filling factor for (B), (C) is 50 %.

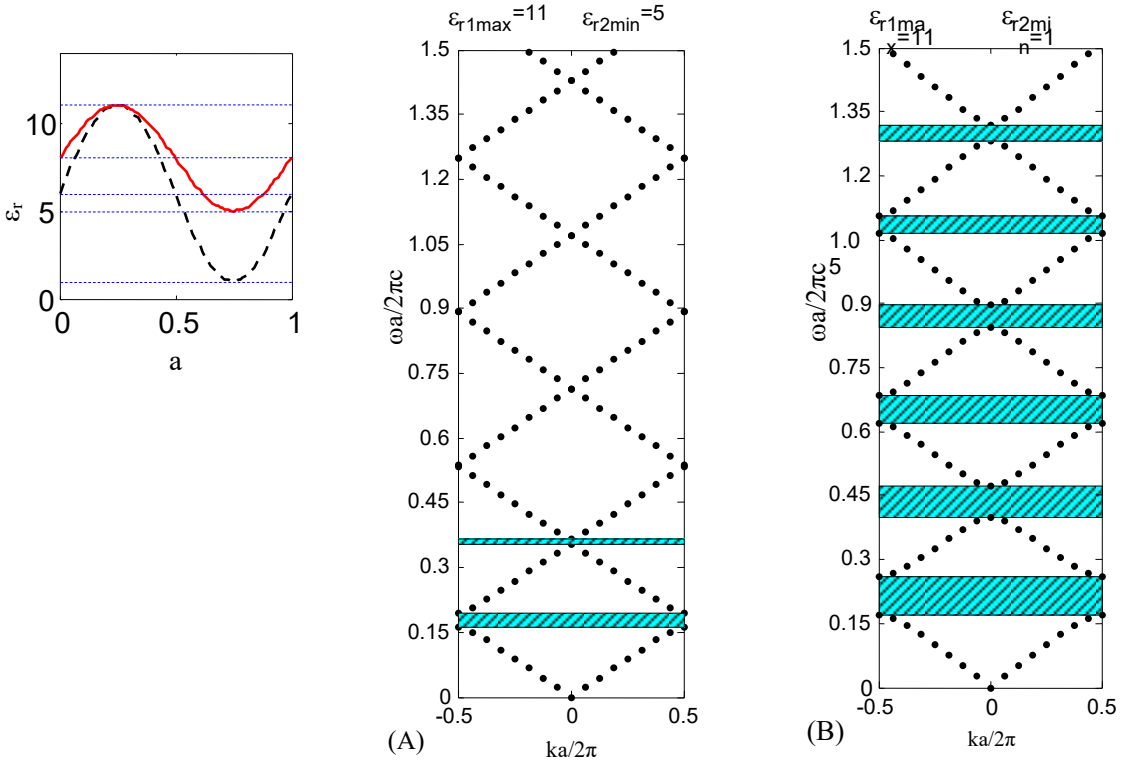

Fig. 3. Unlike Fig. 2 where the refraction indices alternate each a/2, the two diagrams (on the right) show the forbidden bands of two 1D crystals having a sinusoidal variation for ε_r. In the first case, (A) (ε_{rmax}=11, ε_{rmin}=5) and for the second, (B), (ε_{rmax}=11, ε_{rmin}=1). Again, as the amplitude of the sinusoid varies in a larger interval, the gaps size grows.

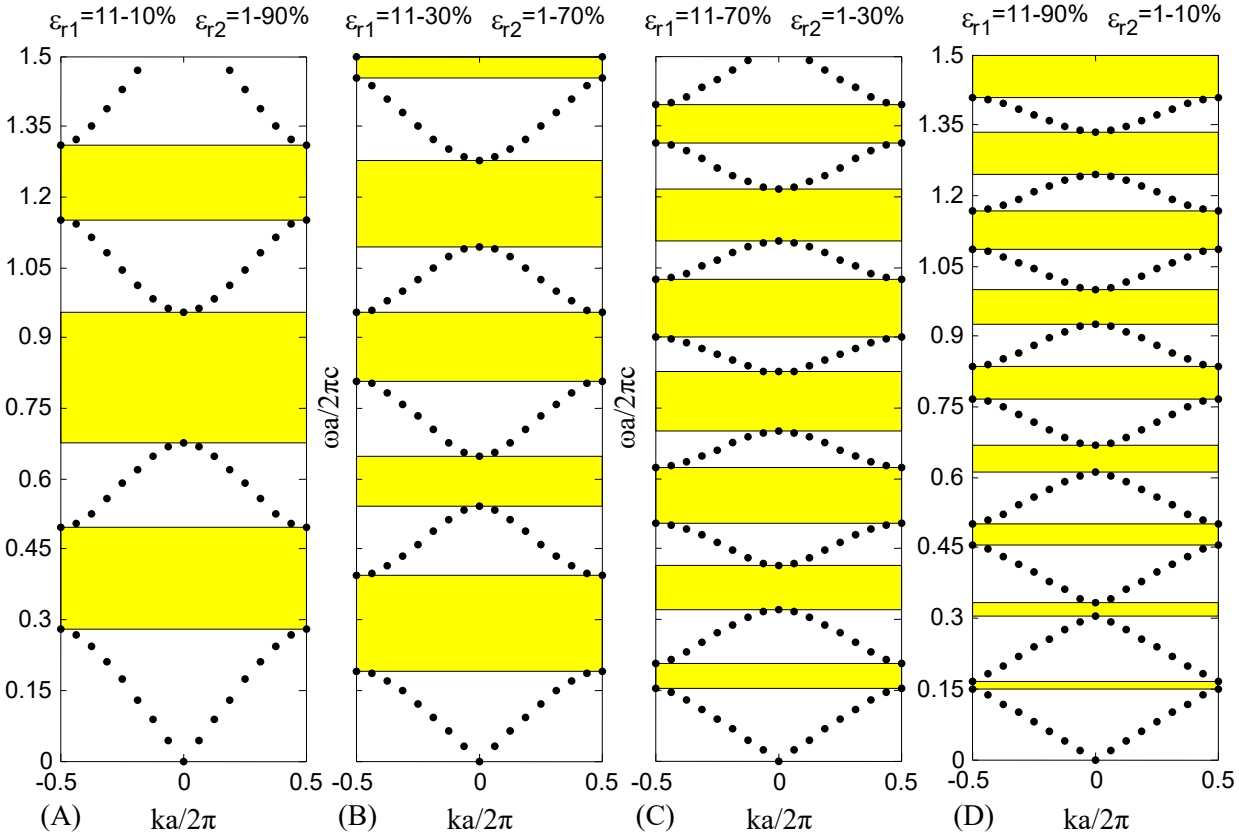

Fig. 4. The four diagrams present the influence of the filling factor on the gaps width and the number of forbidden bands. Again two alternating media, like in Fig. 2, are considered. As a remark, the gaps are large and reduced in number if the substance with ε_r=11 occupies a small proportion of the period a. On the contrary, if the medium having ε_r=1 is the one in minority, the number of forbidden bands is larger but the extent of each one diminishes.

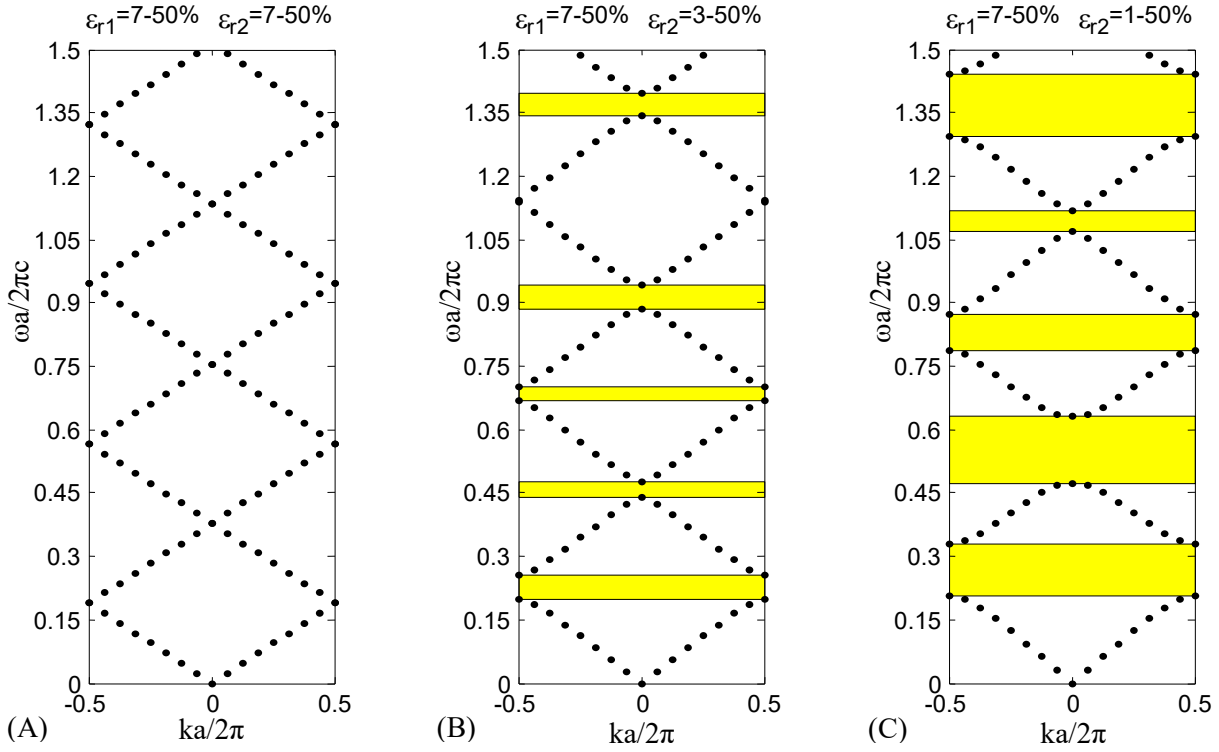

Fig. 5. (A). The band structure of a homogeneous medium having $\varepsilon_r=7$. There are no forbidden domains. (B) The band gaps of a multilayer with two alternating strata: $\varepsilon_{r1}=7$ and $\varepsilon_{r2}=3$. (C) The bands profile for the case where the two substances are characterized by: $\varepsilon_{r1}=7$ and $\varepsilon_{r2}=1$. The filling factor for (B), (C) is 50 %. Remark: As compared with Fig. 2, either the number of band gaps or their size decreases.

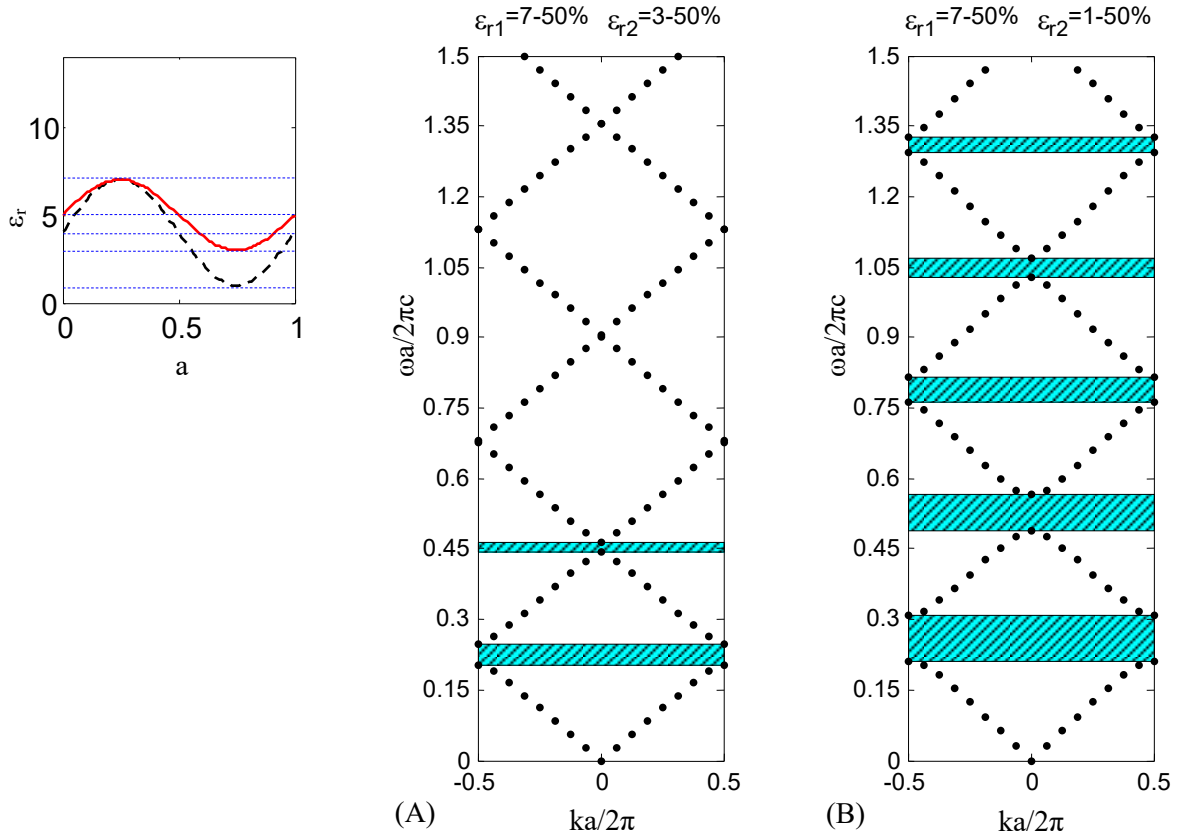

Fig. 6. Again, unlike Fig. 2 where the refraction indices alternate each a/2, the two diagrams (on the right) show the forbidden bands of two 1D crystals having a sinusoidal variation for ε_r. In the first case, (A) ($\varepsilon_{rmax}=7$, $\varepsilon_{rmin}=3$) and for the second, (B), ($\varepsilon_{rmax}=7$, $\varepsilon_{rmin}=1$). Again, as the amplitude of the sinusoid varies in a larger interval, the gaps size grows. However, as compared with Fig. 3, either the number of band gaps or their size decreases.

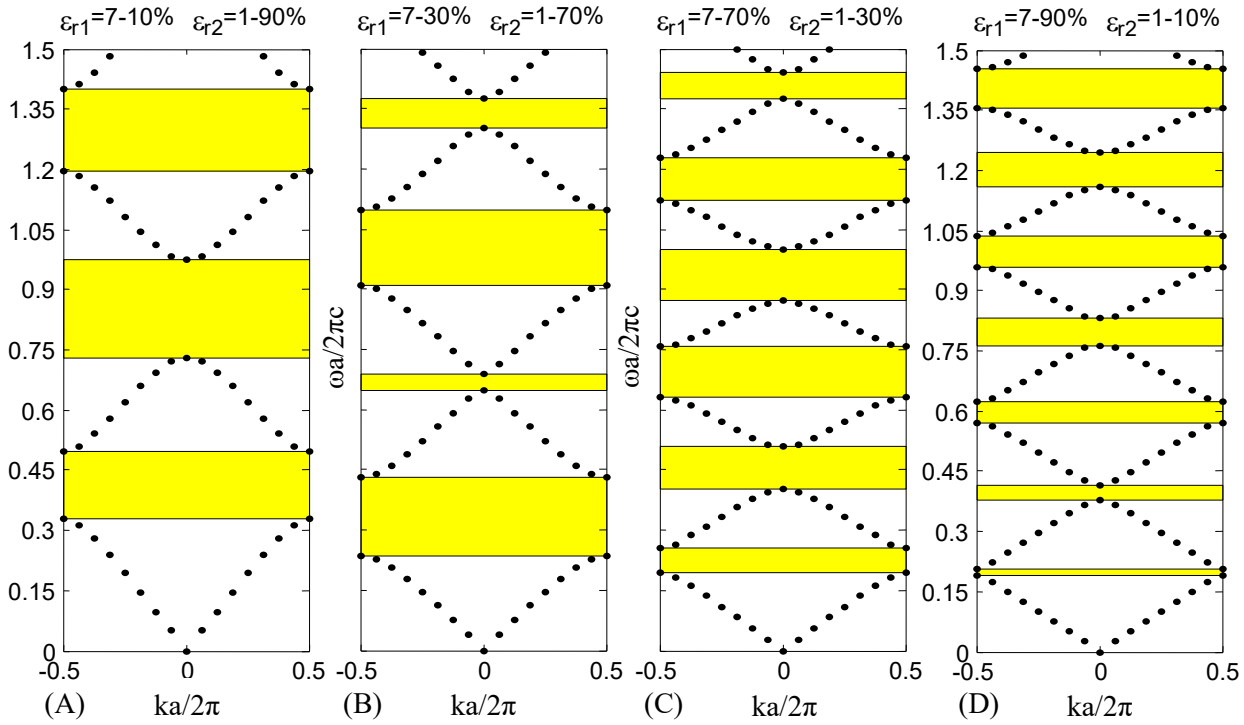

Fig. 7. The four diagrams present the influence of the filling factor on the gaps width and on the number of forbidden bands. Again, two alternating media, like in Fig. 5, are considered. As a remark, the gaps are large and reduced in number if the substance with $\varepsilon_r=7$ occupies a small percent of the period a. On the contrary, if the medium having $\varepsilon_r=1$ is the one in minority, the number of forbidden bands is larger but the extent of each one diminishes. However, the overall performance of the structure is slightly inferior as compared to Fig. 4 either from the gaps size point of view or their number.

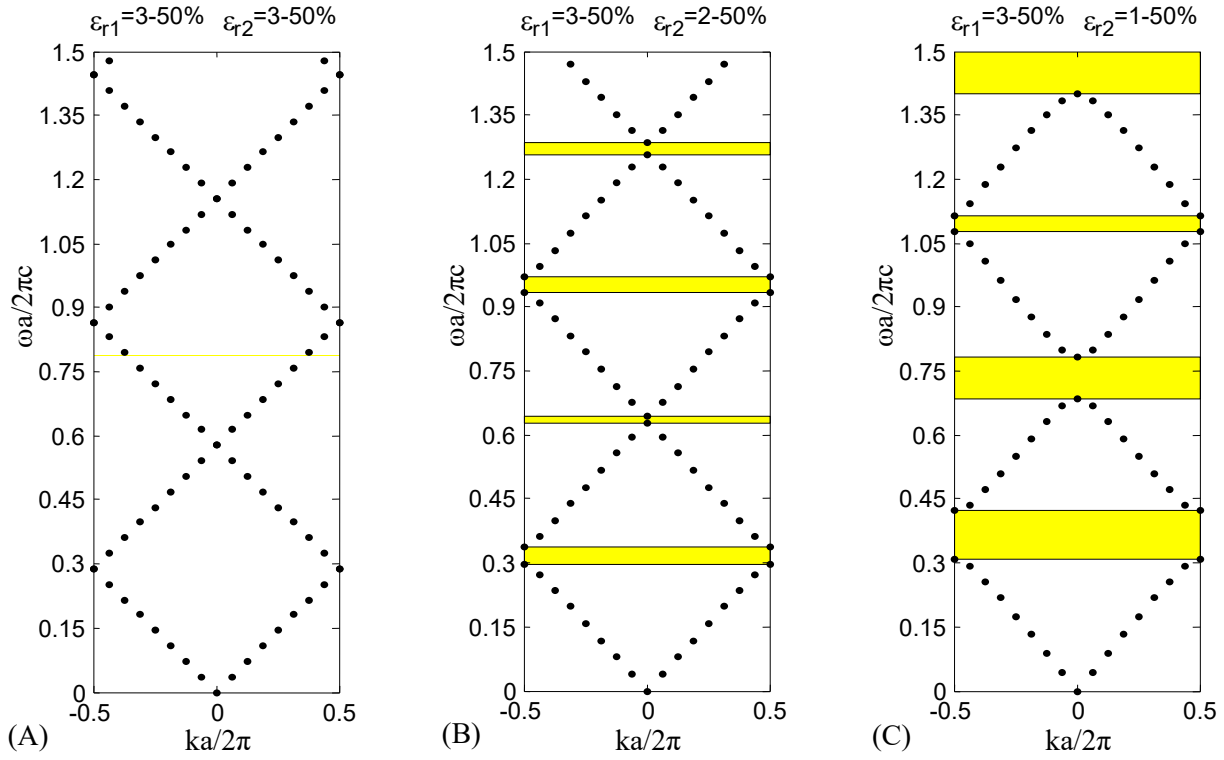

Fig. 8. (A). The band structure of a homogeneous medium having $\varepsilon_r=3$. There are no forbidden domains. (B) The band gaps of a multilayer with two alternating strata: $\varepsilon_{r1}=3$ şi $\varepsilon_{r2}=2$. (C) The bands profile for the case where the two substances are characterized by: $\varepsilon_{r1}=3$ and $\varepsilon_{r2}=1$. The filling factor for (B), (C) is 50 %. Remark: As compared with Fig. 5. either the number of band gaps or their size decreases.

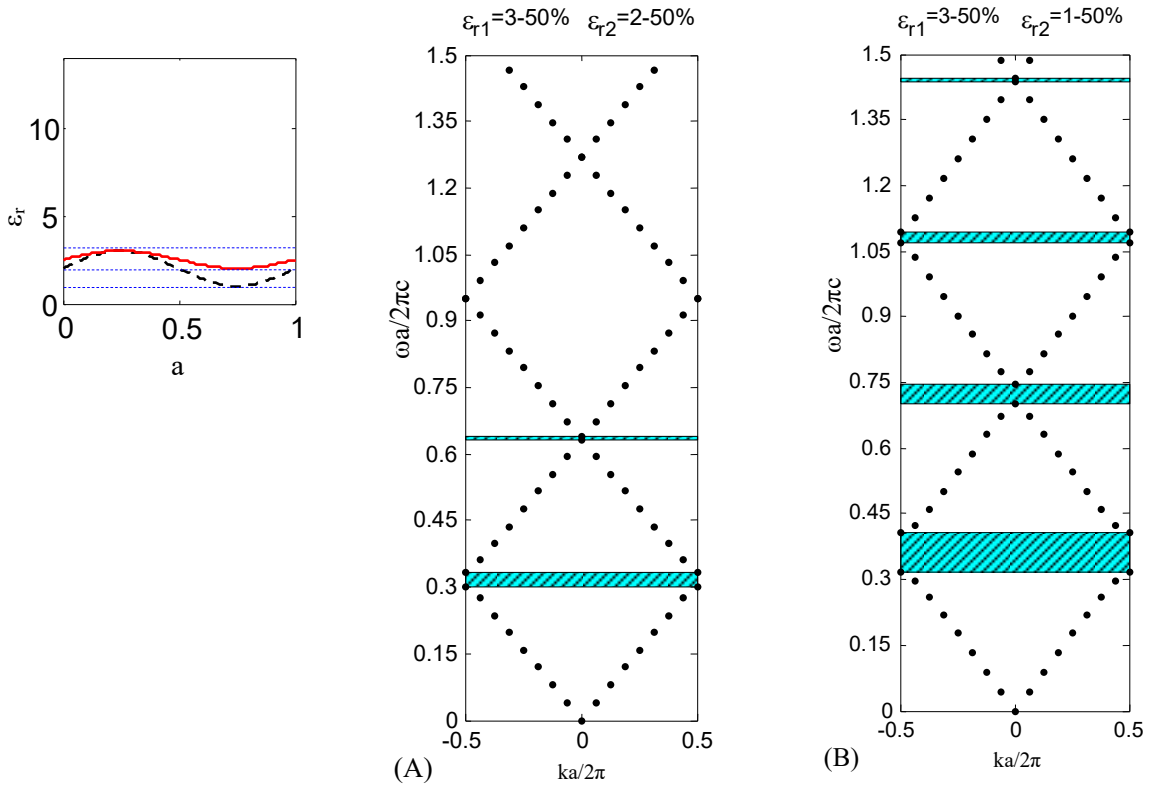

Fig. 9. Once again, unlike Fig. where the refraction indices alternate each a/2, the two diagrams (on the right) show the forbidden bands of two 1D crystals having sinusoidal variation for ε_r. In the first case, (A) (ε_{rmax}=3, ε_{rmin}=2) and for the second, (B), (ε_{rmax}=3, ε_{rmin}=1). Again, as the amplitude of the sinusoid varies in a larger interval, the gaps size grows. However, as compared with Fig. 6, either the number of band gaps or their size decreases.

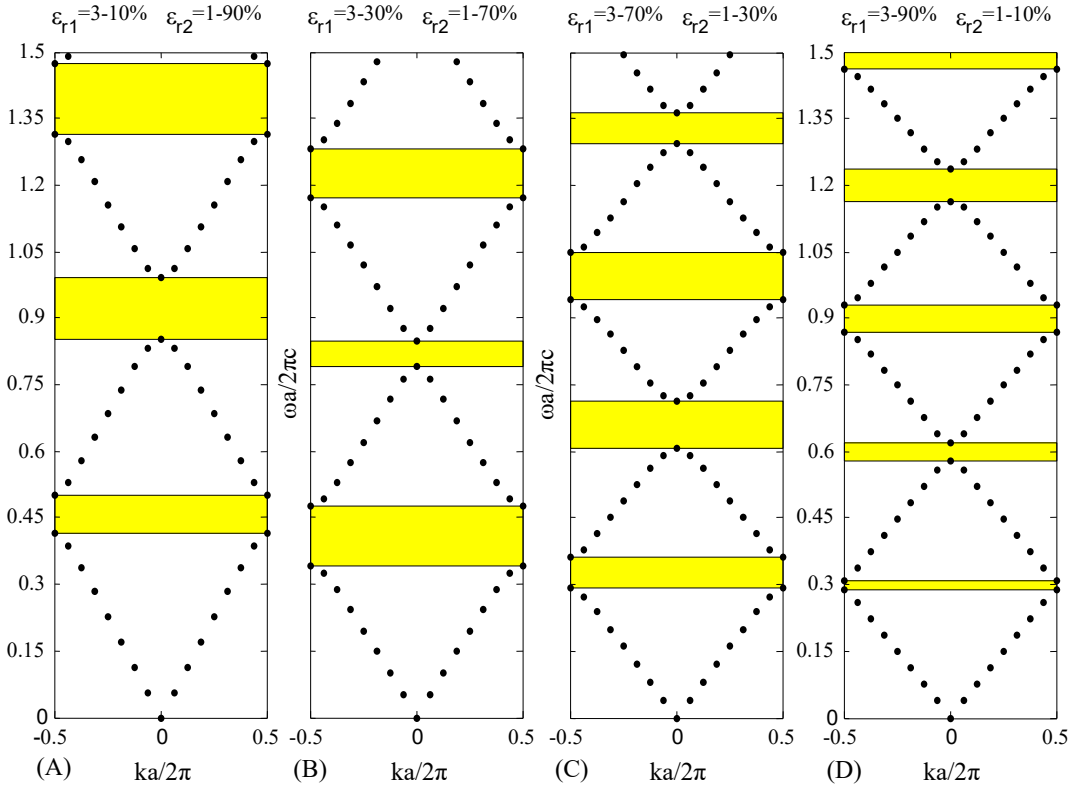

Fig. 10. The four diagrams present the influence of the filling factor on the gaps width and on the number of forbidden bands. Again, two alternating media, like in Fig. 8, are considered. As a remark, the gaps are large and reduced in number if the substance with ε_r=3 occupies a small percent of the period a. On the contrary, if the medium having ε_r=1 is the one in minority, the number of forbidden bands is larger but the extent of each one diminishes. However, the overall performance of the structure is inferior in respect to Fig. 7 either from the

gaps size point of view or their number.

4. The 1D photonic crystal and the periodic defects

Till now, the dependence of the band gaps size and their number versus the contrast and filling factor was investigated. It is time now to push the study a step forward and see what happens if periodic defects are implanted in the crystal. The introduction of such impurities turns the repetitive alternance of period *a*, in a structure also repetitive but having the period equal to the distance between two defects [6]. It have to be said that as the distance between two adjacent doping elements increases, more and more samples are needed and in consequence the quantity of Fourier coefficients p_n (see the theoretical paragraph), grows considerably and so does the number of equations that make the system (15). Solving such large group of equations requires a lot of computer resources and the calculations become prohibitive quickly.

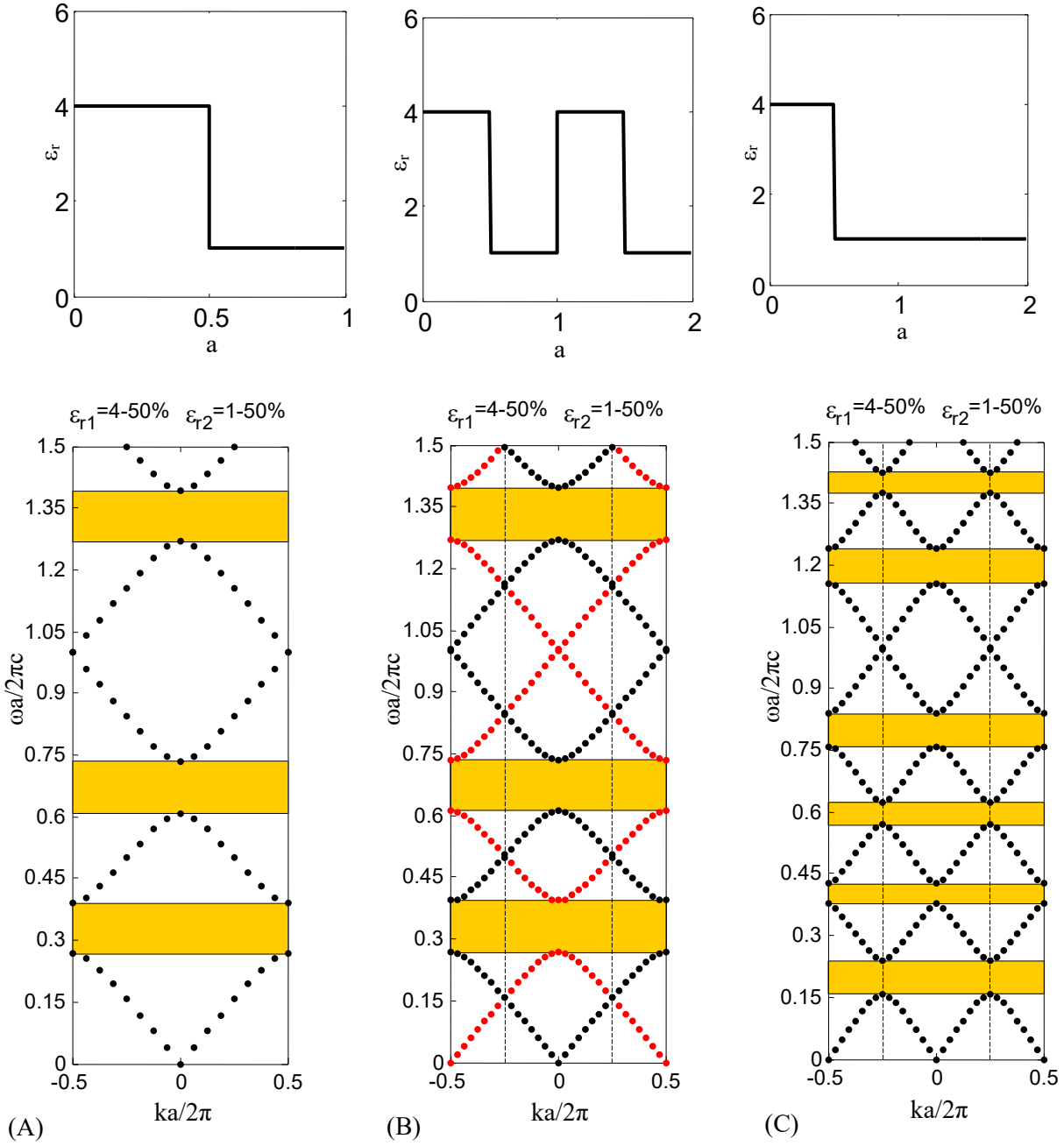

Fig. 11. (A) The band structure of a binary medium with the period, a, having two layers characterized by $\varepsilon_{r1}=4$ and $\varepsilon_{r2}=1$. (B) The band gaps of the same composite, calculated by assuming that the period would be 2a. (C) The structure of forbidden domains for the base crystal described by (A) or (B), but doped with a defect which repeats each two periods (one alternance is missing). Note: the filling factor is 50%.

Remark: The two diagrams (A) and (B) in Fig. 11 correspond to the same entity (1D crystal without defects) and as a result they have to be identical, a fact that is easily proven by comparing the position and size of the band gaps and the correspondence between k and ω, in both diagrams. The dotted black curves match each other. However a new set of solutions appears in (B) (the gray, or red curves in the color version). Apparently, the presence of them is illogical. However, if the periodicity is slightly altered with a small impurity somewhere inside the $2a$ interval, the repetitive structure turns in a new one where the (minimum) period is truly $2a$. The "intersection" points will disappear and tiny band gaps similar with the one in (C) will show up. In consequence, (B) can be considered as a limit circumstance where the prohibited domains from the intersections of the two graphics (red and black) are of zero width. Also, the presence of (B) diagram is not absolutely necessary. For the shake of clarity, an explanation had to be given because the differences between (A) and (C) look semnificative and apparently inexplicable.

Once the clarifications above have been made we can proceed to studying the dependence of the forbidden bands number and of their size on the distance between two adjacent periodic defects. For all situations described below, the definition of "defect" will be: *the absence of one alternance of the substance with* $\varepsilon_r=4$.

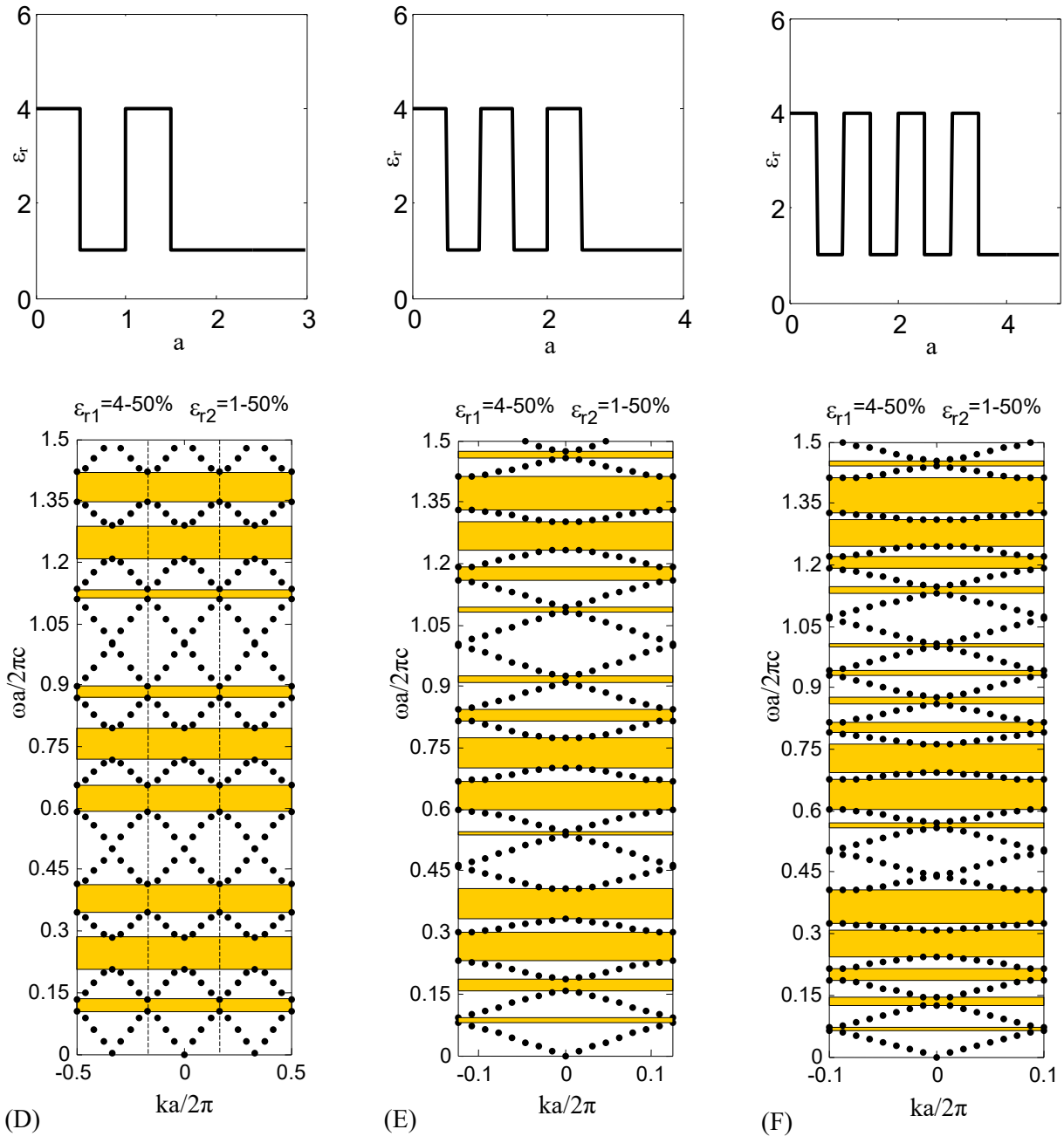

Fig. 12. The structure of band gaps for the crystal in Fig. 11 (A, B) perturbed after: (D) two (E) three, (F) four periods.

It is expected that, as the distance between two consecutive defects become greater and greater, the configuration of band gaps tends to the one of the unperturbed 1D crystal (Fig. 11 A, B). The case, analyzed in Fig. 11 (C) where the inhomogeneity repeats each two periods, leads to a structure with very different properties from the (A, B) circumstance and as a result the prohibited domains of (C) do not mach at all the ones of the undisturbed crystal. If we analyze the diagrams in Fig. 12 and Fig. 13 a convergence to Fig. 11 (A, B) can be noted. Thus, in Fig. 11 (C), six bands similar in size appears, in Fig. 12 (D) nine, and starting from Fig. 12 (E) the gaps, also in quite a large number, starts to grope around the three principal forbidden bands of Fig. 11 (A, B).

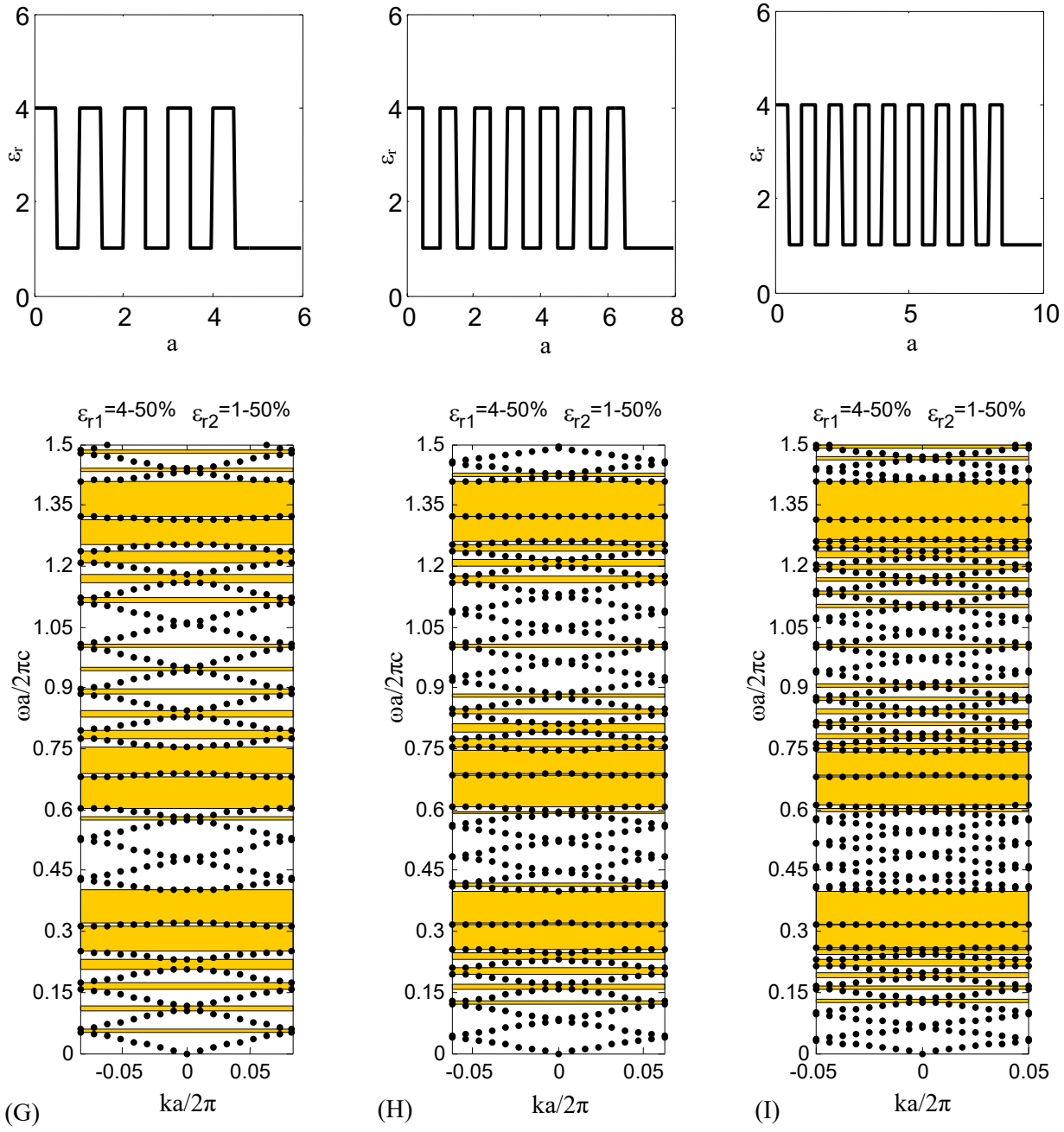

Fig. 13. The structure of band gaps for the crystal in Fig. 11 (A, B) perturbed after: (G) fife (E) seven, (F) nine periods.

A remarkable fact is the apparition of tiny allowed bands (Fig. 13) in the space fully occupied by gaps corresponding to the perfect, unperturbed crystal Fig. 11 (A, B).

As a comment, in Fig. 12 (E, F) and Fig. 13 (G, H, I), 1102epresentation with $ka/2\pi \in [-0.5, 0.5]$ was abandoned because as the length of the period grows to *2a, 3a, 4a*, etc. the periodicity interval in the *k* space decreases to [*-0.25, 0.25*], [*-0.168, 0.168*], [*-0.125, 0.125*], etc.

5. The sensitivity to fabrication errors

In the previous graphical representations *k* and *f* have been normalized to *a*, a fact that hides the real length of the period. If we wish to obtain band gaps for the optical domain then *a* must be in the range of hundreds of nanometers. Manufacturing such thin layers involve inherent fabrication errors and as a consequence a detailed analyze having the purpose to study the influence of errors over the width, size and position changes of the ideal band gaps, is needed.

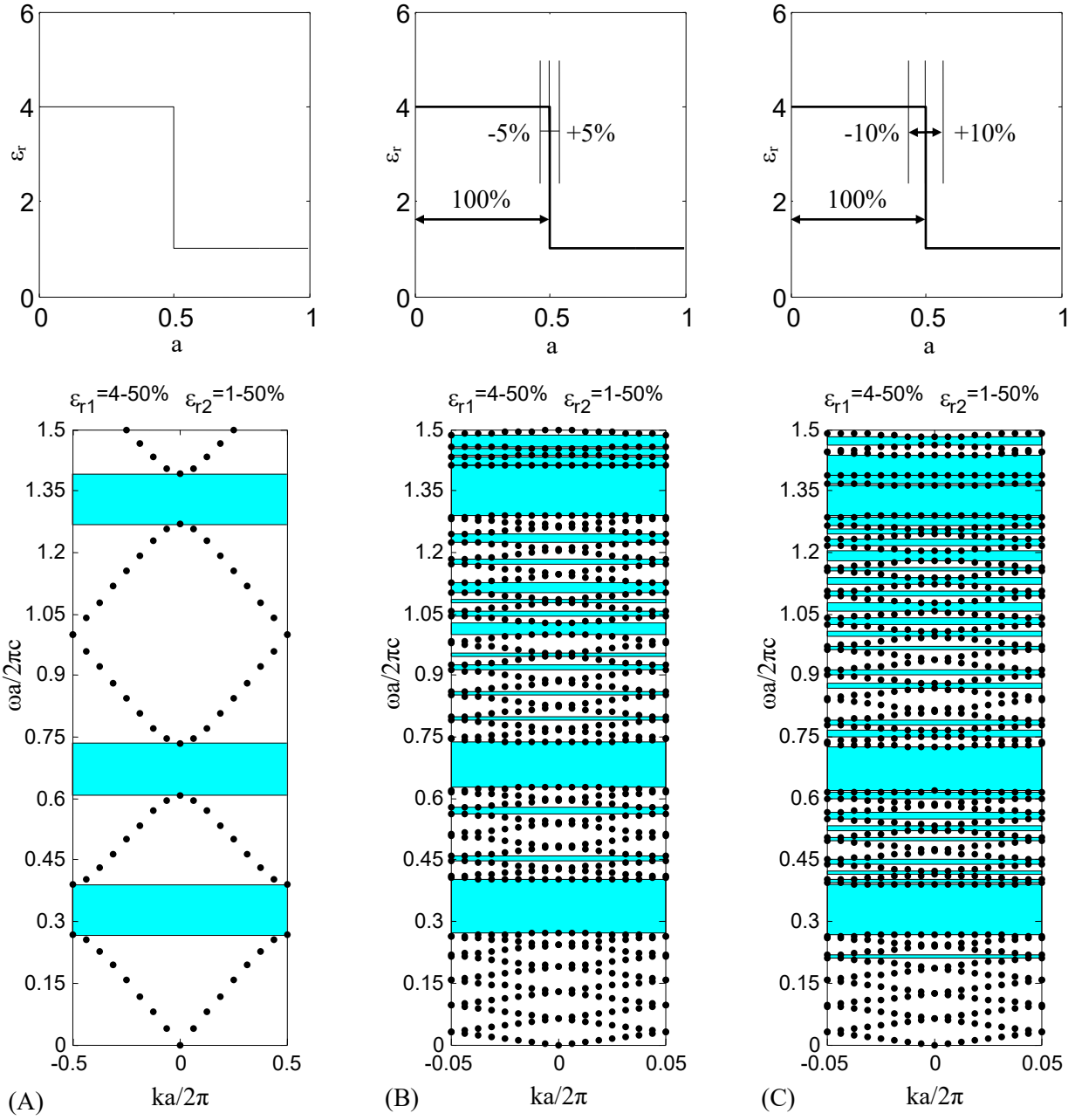

Fig. 14. (A) The structure of band gaps for a binary medium having the period a and two layers with permittivity $\varepsilon_{r1}=4$ and $\varepsilon_{r2}=1$. (B) The forbidden bands of the same crystal where the width of the strata varies in the limit of ±5%. (C) Same as (B), the only difference is that the tolerance increase to ±10%.

Fig. 14 (B) and (C) shows that, as the fabrication errors are larger and larger, the band structure deteriorates, changes, as compared to the ideal case of zero tolerance from Fig. 14 (A). *A good point is that, the three band gaps, maintain with a good approximation, their position and width. However, a lot of forbidden domains appear in the allowed space of the ideal structure.*

If for instance the composite is used to stop radiation in a certain frequency range without taking care of what happens outside that domain, then the additional band

gaps do not matter. For other applications the consequences might be negative.

Remark: In order to satisfy the conditions for which the algorithm in the theoretical paragraph can be used, the diagrams in Fig. 14 (B, C). It is used the assumption that the random errors take place along ten periods *a* and after that the entire pattern repeats to infinity.

5. Conclusions

The mathematical procedure described in the theoretical paragraph and used along the present paper, for obtaining all the numerical results, is well suited for studying the influence of factors like: filling percentage, contrast, error sensitivity, on the band structure of 1D crystals.

As the contrast (defined like $\varepsilon_{rhigh}/\ \varepsilon_{rlow}$) increases the number of band gaps gradually diminishes but their width grows considerably, large forbidden bands being obtained for succession of materials where one has a relative permittivity as large as possible while the other the minimum. Another remark is that for wide gaps, abrupt changes in permittivity are needed. Smooth variations from ε_{rhigh} to ε_{rlow} do not bring good results.

Filling factor (the percentage occupied by one of the substances) also, greatly influences the band structure and the size of the gaps. The forbidden domains are large and reduced in number if the material with ε_{rhigh} occupies a small percent of the period *a*. On the contrary, if the medium having ε_{rlow} is in minority, the number of band gaps is larger but the extent of each one diminishes.

References

[1] K. M. Leung, Y. F. Liu, Physical Review B, **41**(14):10188-10190, 1990.
[2] S. Johnson, J. D. Joannopoulos, Kluwer Academic Publisher, Norwell, Massachusetts USA, 2002.
[3] J. D. Joannopoulos, R. Meade, J. Winn, Princeton University Press, Princeton, 1995.
[4] K. M. Ho, C. T. Chan, C. M. Soukoulis, Physical Review Letters, **65**(25), 3152 (1990).
[5] G. Guida, PIER - Progress in electromagnetic research, **41**, 107 (2003).
[6] Rossella Zoli, Marco Gnan, Davide Castaldini, Gaetano Bellanca, Paolo Bassi, Optics Express 2905 **11**(22), 3 (2003).

*Corresponding author: sterian@physics.pub.ro